Progress In Electromagnetics Research M, Vol. 80, 71–81, 2019

Flexible UWB AMC Antenna for Early Stage Skin Cancer Identification

Ameni Mersani[1, *], Lotfi Osman[1], and Jean-Marc Ribero[2]

Abstract—This work involves designing an antenna that meets the requirements of radar systems. The associated technology, which was for a long time reserved for the military field, is now available in the civil field, as well as in the biomedical sector for the development of "monitoring" systems allowing to monitor the state of health of a patient in a non-invasive way. The goal of this article is to design a wearable textile antenna to detect cancerous tumors of a patient without direct contact with the skin taking into account the electromagnetic waves directed towards the human body due to the difference between the dielectric constants of healthy and unhealthy tissues. Here we present a miniature AMC antenna of rectangular shape that satisfies the UWB characteristics in terms of bandwidth and reflection coefficient. The proposed AMC antenna operates in X-frequency band (8–12 GHz). Using a model of dielectric artificial skin, we have simulated the specific absorption rate on the human body in order to better respect the FCC standards allowed 1.6 W/kg averaged to 1 g of human tissue.

1. INTRODUCTION

Ultra-wideband (UWB) transmission seems to be a very promising technology for ultra-fast wireless communications, high-precision radars, and imaging systems. The UWB technology that was originally used in military applications is nowadays exploited by various applications, since its authorization by the American Federal Commission of Communications (FCC) in February 2002.

The FCC has established certain regulations for the bands of frequencies and transmission power limits, allocated to various UWB applications. Accordingly, any system with a fractional bandwidth of at least 20% or a bandwidth of at least 500 MHz may be considered a UWB transmitter [1]. In recent years, among the various UWB applications, microwave medical imaging has attracted considerable interest. Wearable technology is a growing potential field that will reduce medical errors and improve the quality of healthcare in hospitals. Every year, there are a lot of dangerous and deadly diseases and infections that require screening tests to save lives [2]. Xeroderma pigmentosum is an inherited disease of a rare genetic origin. It is characterized by an excessive skin sensitivity and a very high risk of developing skin cancer [3]. Melanoma is a serious form of skin cancer originating from the pigment-producing cells (melanocytes). These cells become abnormal, grow uncontrollably, and aggressively invade surrounding tissues. The growth of the melanoma results in a local variation of permittivity and electrical conductivity of the skin tissue that can be monitored to estimate the extension of anomalous cells by the time. At initial stages, most of the skin cancers are curable, so a prior detection of skin cancer can save the lives of the patients [4–6].

In the literature, there are several works devoted to microwave imaging applications. For example, Khor et al. [7] presented an attractive experimental study, which was able to detect the presence and accurately locate a high permittivity object (simulating the tumour), placed in a cylinder within a low

Received 14 December 2018, Accepted 9 March 2019, Scheduled 4 April 2019
* Corresponding author: Ameni Mersani (mersani.ameni@gmail.com).
[1] Department of Physics, FST, University of Tunis El Manar, 2092, Tunisia. [2] Department of Electronics, University of Nice Sophia Antipolis, 06903, France.

permittivity plastic (modelling healthy fat tissue) using a Vivaldi type antenna. Caratelli et al. [4] propose a noninvasive micro-sensor system which has adopted a conformal local finite difference time domain enhanced procedure, based on the definition of efficient material parameters and appropriate standardization of magnitudes related to electromagnetic field.

Our goal in this work is to design an antenna aiming to exploit the dielectric-property contrast between normal skin tissue and malignant tumors [8, 9]. There is more water content in tumor tissue than healthy tissues [2]. Narrow beamwidth, high directivity, high gain, and a wide bandwidth are highly essential features of an antenna in a microwave device which can be used for skin cancer detection. Lower frequencies provide deeper penetration while higher frequencies offer better range resolution and less skin depth, and this is the aim of using X-band in this work [2]. Since skin is very sensitive to radiations, radiations can easily penetrate the skin. Therefore, X-band is preferred here so that radiations limit themselves only to the skin level and do not penetrate the muscles as high frequency leads to less skin depth. X-band provides the required skin depth and also a reasonable gain. In recent years, the most common skin cancer diagnosing technique is screening.

Skin cancers cannot be "detected" in the strict sense since we cannot identify them before the appearance of symptoms. As a result, we propose, in this article, a wearable textile antenna that can be integrated into the clothes of a person affected by the xeroderma pigmentosum disease. We aim to detect cancer even before it has manifested symptoms such as abnormal swelling and a dysfunction in the body. The proposed antenna is rectangular and is basically of a low gain, as our first concern is to protect the human body from radiation. Reducing the size is also taken into consideration when designing this antenna, which would make it easier to be integrated into the system and reduce clutter. For this, certain techniques are used [1, 10]. Out of these techniques, we will use the metamaterials. Over the past decades, various artificial magnetic conductors (AMCs) have been presented targeting aspects such as increased gain, direct radiation pattern and reflecting the harmful radiation of the antenna [6, 11].

In [12], researchers propose a thin film-based wearable UWB antenna implemented over an AMC in order to reduce the effect on the human body and improve gain and bandwidth characteristics. In a recent study, a low profile printed slot antenna using a wideband AMC has been presented with improved radiation performance. It achieves a wide impedance bandwidth in the measured frequency range of 7.96–12.56 GHz ($|S_{11}| \leq -10$ dB) for X-band applications [13]. In [14], a novel miniaturized AMC using interdigital capacitors is presented. The proposed prototype provides a bandwidth of 275 MHz (4.4%) around the operating frequency of 6.2 GHz.

The proposed work in this article is the design of a compact AMC based monopole antenna with UWB characteristics, which will be inserted into a skin cancer detection system. It is simulated in the first place using the commercial software package CST Microwave Studio environment to realize a prototype thereafter

In the context of communications near the human body, the problems are changes in the characteristics of the antenna due to the proximity of the antenna because it causes the absorption of energy in the human body. The back radiation is most important and will induce radiation absorbed by the human body. This harmful radiation can be quantified by measuring the Specific Absorption Rate (SAR). It is, therefore, necessary to evaluate and quantify the impact of the antenna on the human body. The effect of bending on the antenna performance is also tested.

2. ANTENNA DESIGN

The geometry of the studied monopole antenna is shown in Figure 1. This antenna was simulated, optimized, and printed on a flexible textile substrate.

The used substrate is Felt (dielectric permittivity $\varepsilon_r = 1.22$, $\tan\delta = 0.016$, and thickness $h = 2$ mm) [18, 20], and it is of dimensions $L = 36$ mm and $W = 32$ mm. The electro-textile is Zelt, which is a tin/copper coated plain weave, and has a high quality nylon-based substrate offering a better protective fabric with a conductivity of 1×10^6 S/m and a thickness of 0.06 mm. Zelt is also flexible for deformation. This monopole is powered by a 50 Ohm CPW coplanar microstrip line. Table 1 shows the dimensions of the proposed antenna. The substrate and electro-textile are cheap, and therefore the antenna has low cost.

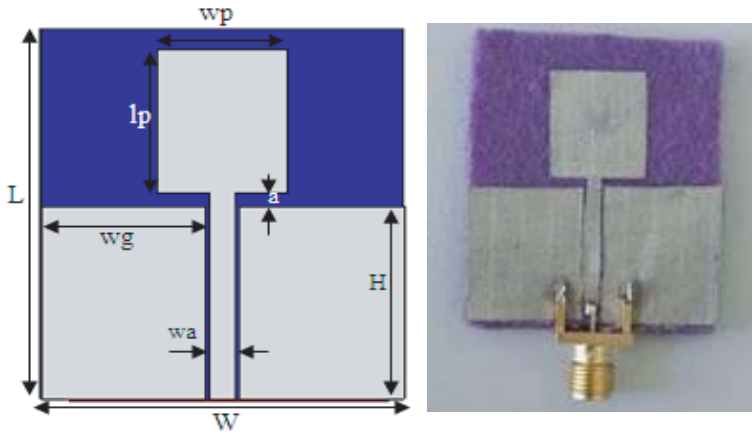

Figure 1. Geometry of the patch antenna.

Table 1. Dimensions of the antenna.

Parameters	Value (mm)	Parameters	Value (mm)
W	32	Wg	14.8
L	36	Wa	2.2
Lp	14	H	18.75
Wp	11.5	a	1

The used simulation tool is the Computer Simulation Technology-Microwave Studio (CST) which is based on the Finite Integration Method (FIT).

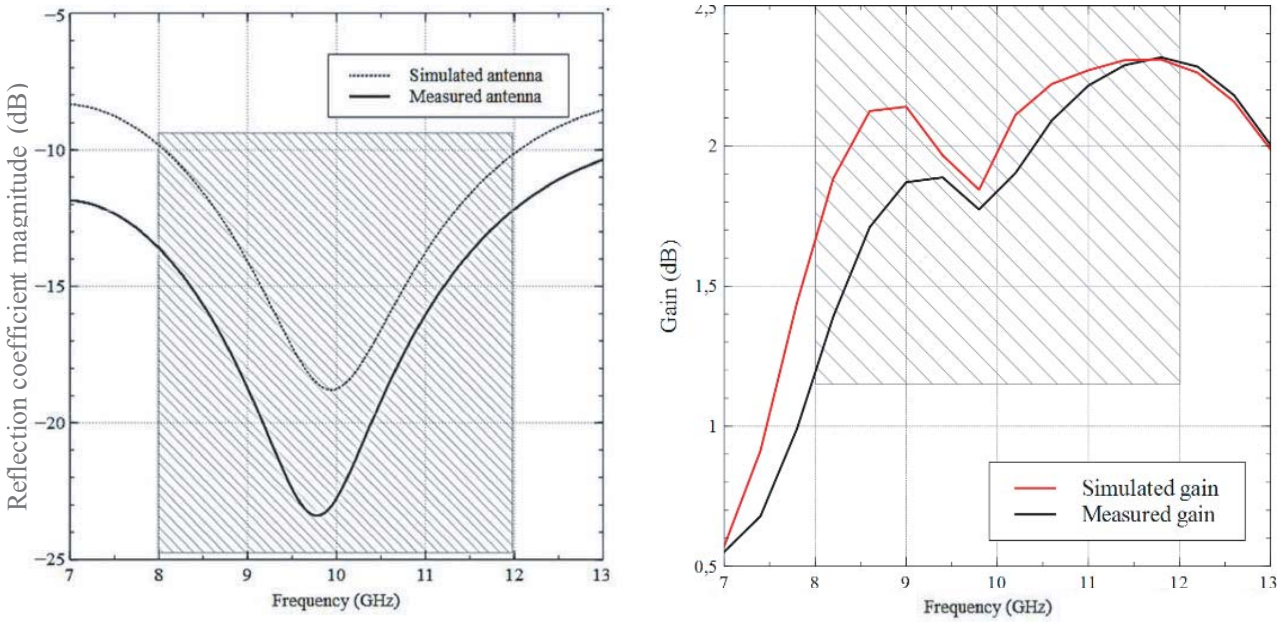

(a) (b)

Figure 2. (a) Comparison of $|S_{11}|$ of the monopole antenna. (b) Simulated and measured gain of the monopole antenna.

Figure 2(a) shows the variation of the reflection coefficient magnitude with frequency. The $|S_{11}|$ value of this antenna shows an impedance bandwidth, measured at -10 dB, ranging from 8 GHz to 12 GHz and a bandwidth of 4 GHz that shows a good adaptation at X-band for both simulated and measured results. The reflection coefficient magnitude $|S_{11}|$ of the antenna shows a slight difference between the simulation and measurement resulting from the imperfect realization.

Figure 2(b) gives the variation of antenna's gain. It happens to be between 1.8 dB and 2.3 dB on the frequency band that we are interested in, which is 8–12 GHz.

Also, we present, in Figure 3, 2D radiation patterns of the antenna for respective frequencies 8 GHz, 10 GHz, and 12 GHz. We note that the antenna has an omnidirectional behaviour in both planes (E and H) for the three frequencies.

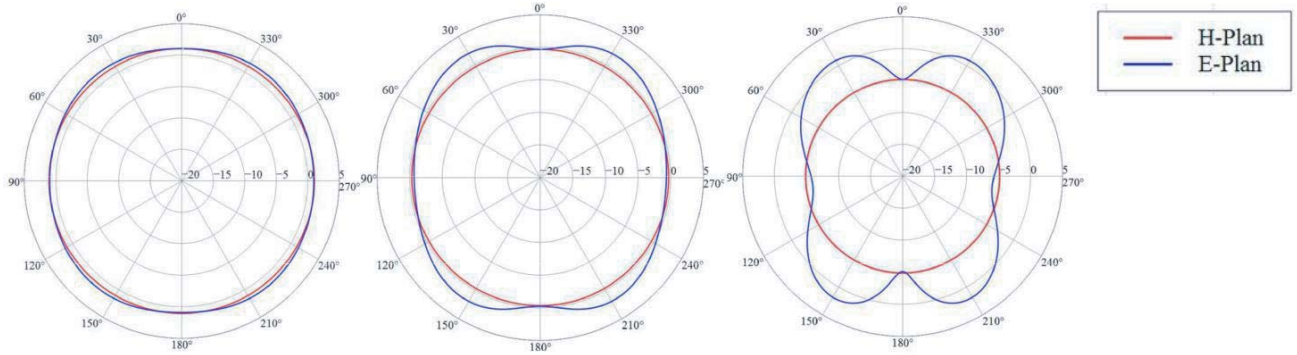

Figure 3. Radiation patterns at (a) 8 GHz, (b) 10 GHz, (c) 12 GHz.

When an antenna is fabricated, the back radiation can be awkward and further, radiates into the human body when it is nearby. To avoid this, either the back radiation is absorbed (which has the disadvantage of loosing of half of the energy), or reflective planes are used.

In good conditions of use, these planes make it possible not to have back radiation and also double the gain of the antenna whose radiation is reflected. This can be explained by means of image theory.

3. AMC STRUCTURE

AMCs are structured with periodic metallic patterns printed on a dielectric substrate. Generally used as a reflective planes, they have a very interesting property of having a phase of the reflection coefficient varying from $-180°$ to $180°$ passing through $0°$, unlike the conventional ground plane, which admits a reflection of $180°$. This phase property is very important because it reduces the size of the antenna compared to a conventional ground plane.

Here we propose a study of a UWB AMC based on square conductive elements with annularly shaped slots. This part will be used to understand the operating bases of the AMC, using its LC equivalent model. This will especially evaluate the performance and size of the cells for our application. This cell has been obtained from the work of Sievenpiper [6].

The studied AMC cell of dimension L is represented in Figure 4. It consists of a square patch of width w with an annular slot engraved on a textile substrate Felt of thickness "a".

An AMC cell based on square patches with a slot is modelled analytically by an LC circuit with a resonant frequency of $1/(2\pi\sqrt{\mathrm{LC}})$ and the characteristic impedance of $\sqrt{(\mathrm{L/C})}$ [6] as shown in Figure 5(a). This circuit constitutes surface impedance Zs whose value depends on the geometry of the cell, the capacitance between the square patches, and the inductance created by the height of the substrate. This modelling gives correct results for cell sizes whose wavelength is much shorter than the period of the cell. The total dimensions of the patch of the unit cell are 11×11 mm. By adjusting the radii dimension R and $R1$, the AMC bandwidth can be flexibly controlled.

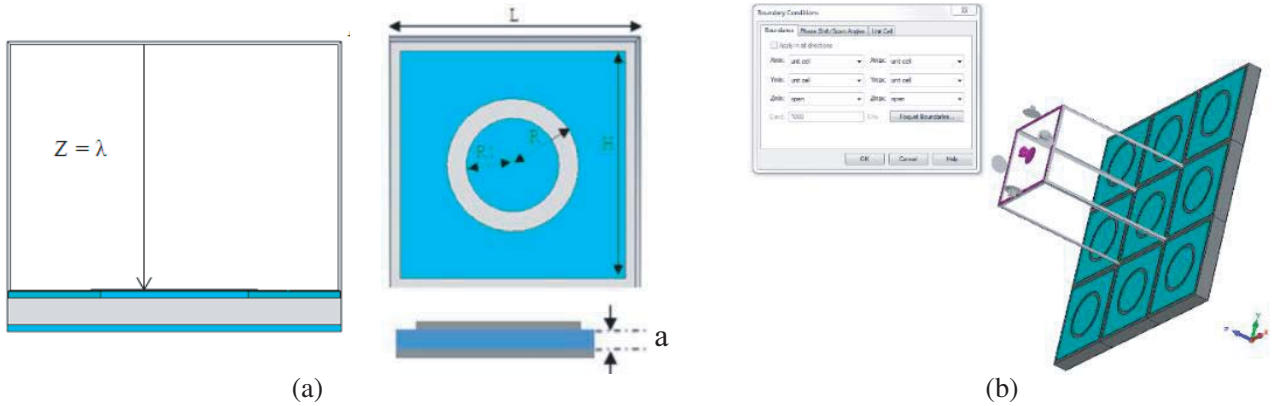

(a) (b)

Figure 4. (a) AMC unit cell ($L = 12\,\text{mm}$, $H = 11\,\text{mm}$, $R = 3.5\,\text{mm}$, $R1 = 3\,\text{mm}$, $a = 2\,\text{mm}$). (b) Configuration of the environment setup for AMC reflection phase in the CST simulation.

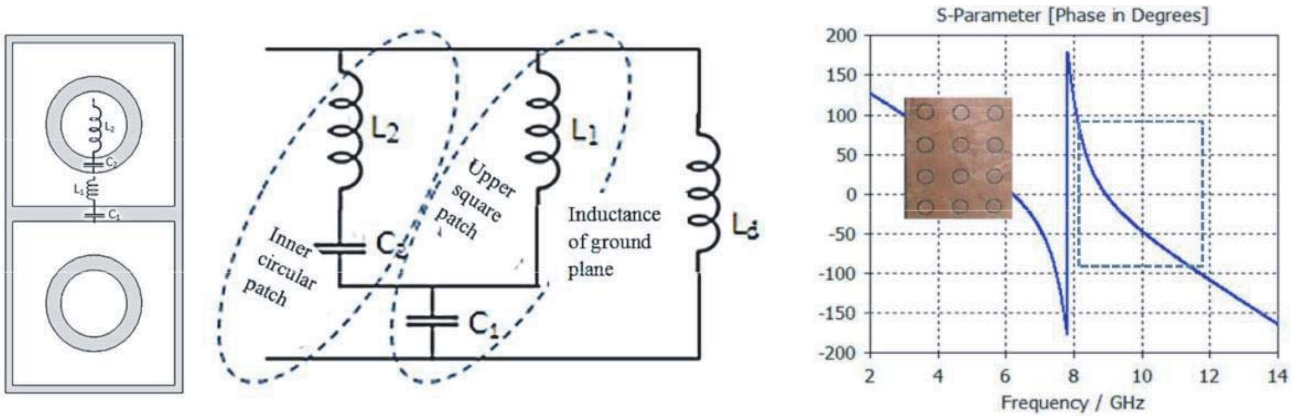

(a) (b)

Figure 5. (a) Circuit model for the AMC showing the grid and dielectric impedances. (b) Phase of the unit cell reflection coefficient.

In this part, the unit cell is optimized for operation in the X band (8–12 GHz). Figure 5(b) illustrates the phase of the unit cell reflection coefficient as a function of frequency. We can see that the AMC exhibits a behavior that spreads over a wide frequency band for a phase between $-90°$ and $90°$.

4. ANTENNA ABOVE ARTIFICIAL MAGNETIC CONDUCTOR

In Figure 6(a), we present the prototype and fabricated monopole antenna which is placed on the AMC surface with 3 patterns by 4. A 2 mm thick foam layer of permittivity $\varepsilon_r = 1.05$ is combined to avoid the coupling between the AMC and the antenna. Figure 6(b) shows the modulus of the reflection coefficient as a function of frequency. When we compare simulated and measured results, we find a good agreement between them. The observed undulations can be attributed to the lack of precision in carrying out the transmission calibration of the differential measurement procedure.

To evaluate the performance of our wearable AMC antenna on the body, we chose to simulate the structure on a biological tissue model available on CST as shown in Figure 6(c). We note a slight frequency shift of the reflection coefficient S_{11} compared to the measured AMC antenna on free space. This is due to the energy absorption in the body.

The efficiency of the AMC antenna is measured in the 3D bench and compared with a reference antenna. The maximum gain and total efficiency of the antenna in the presence of the AMC are shown in Figures 7(a) and 7(b), respectively. There are some differences between measurement and simulation.

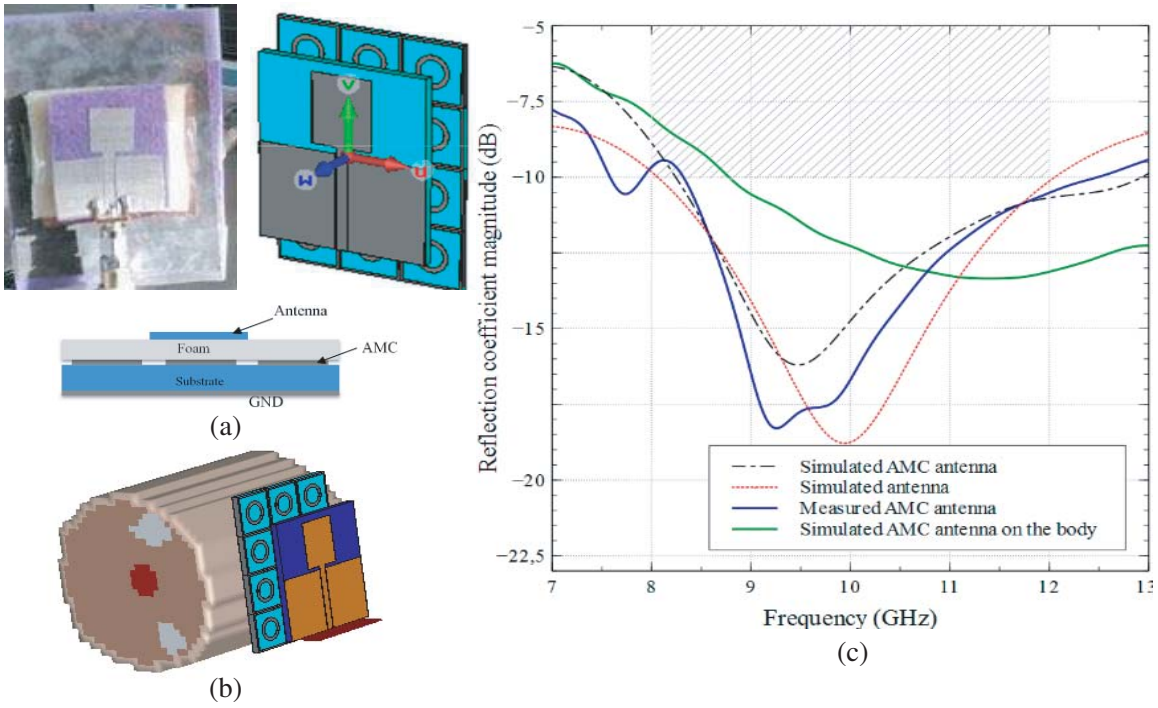

Figure 6. (a) Geometry of the AMC antenna. (b) Simulated and measured of $|S_{11}|$ of the antenna with/without AMC and on the body. (c) AMC antenna on the body.

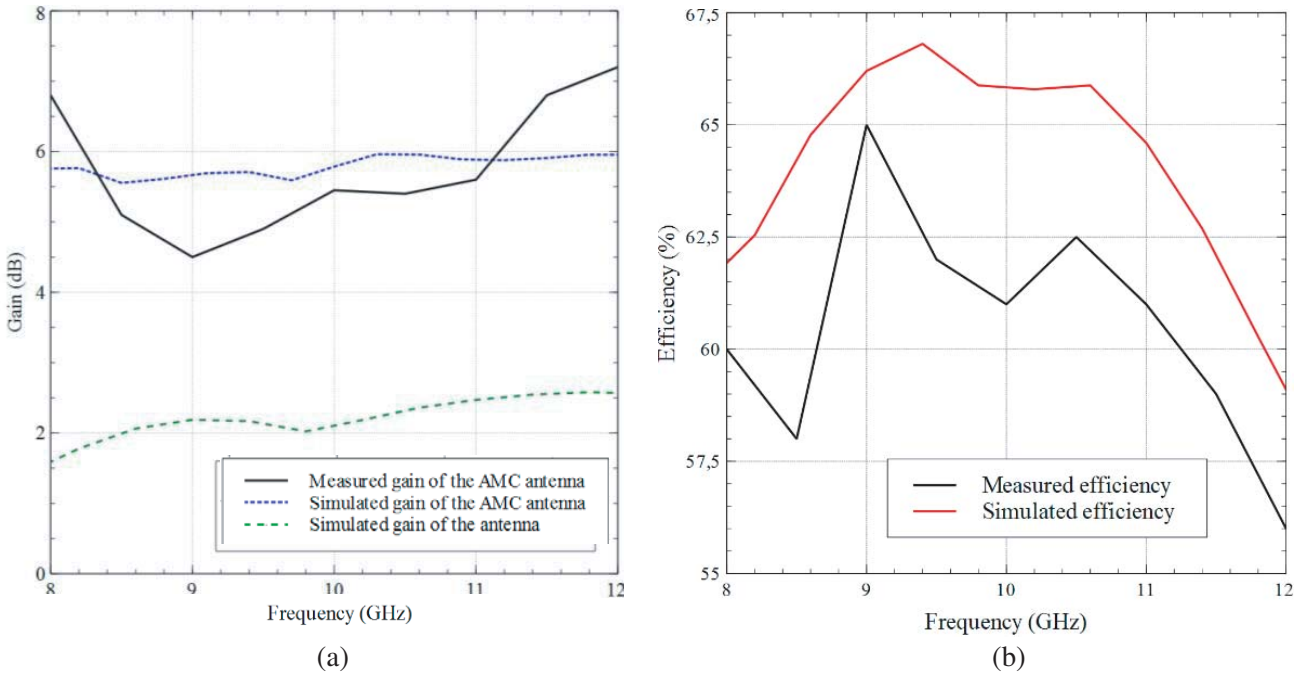

Figure 7. Simulated and measured (a) gain with/without AMC. (b) Efficiency of the monopole antenna with AMC.

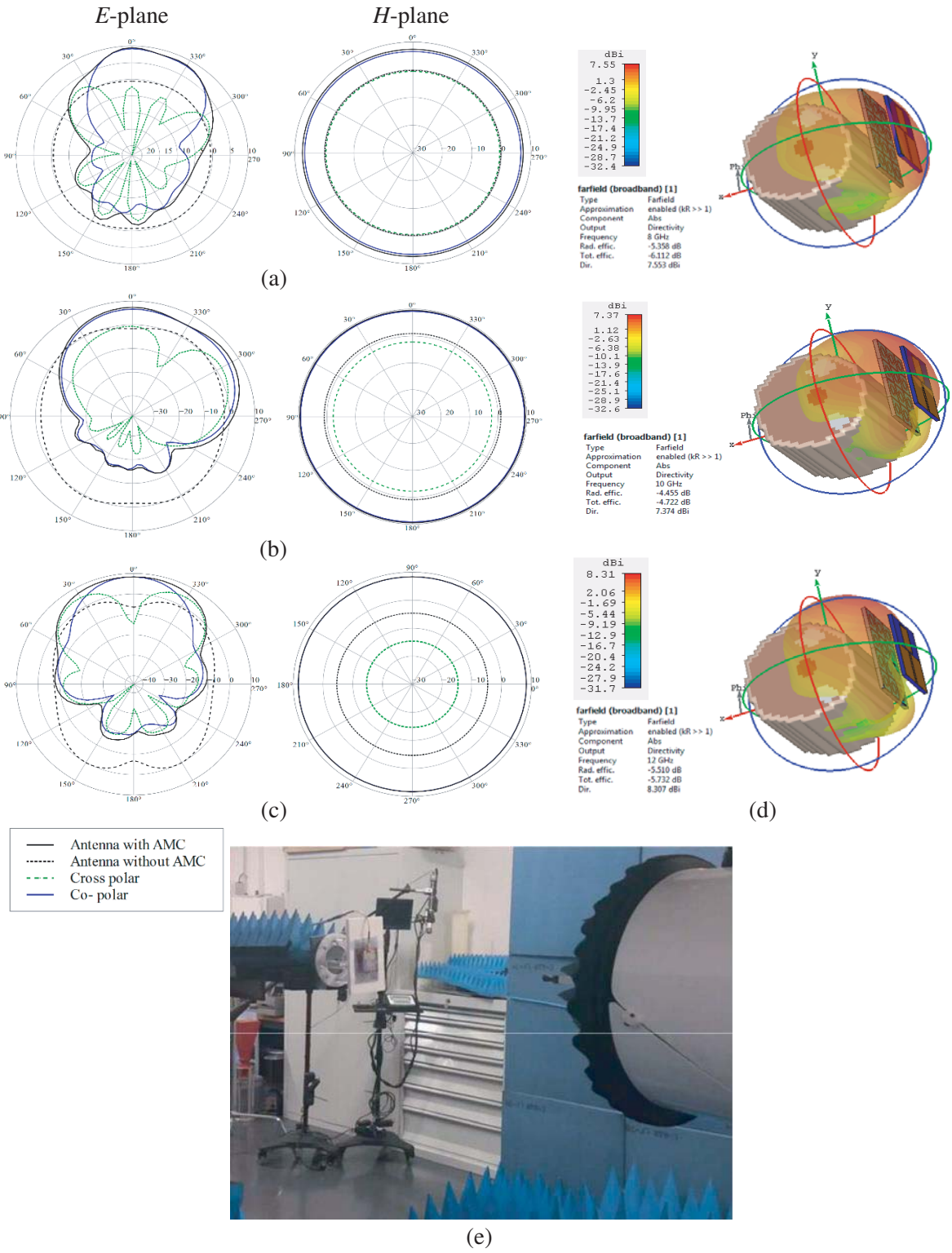

Figure 8. Radiation patterns of the antenna with AMC. (a) 8 GHz, (b) 10 GHz, (c) 12 GHz, (d) on a Biological tissue model, (e) measured AMC antenna on the LEAT anechoic chamber.

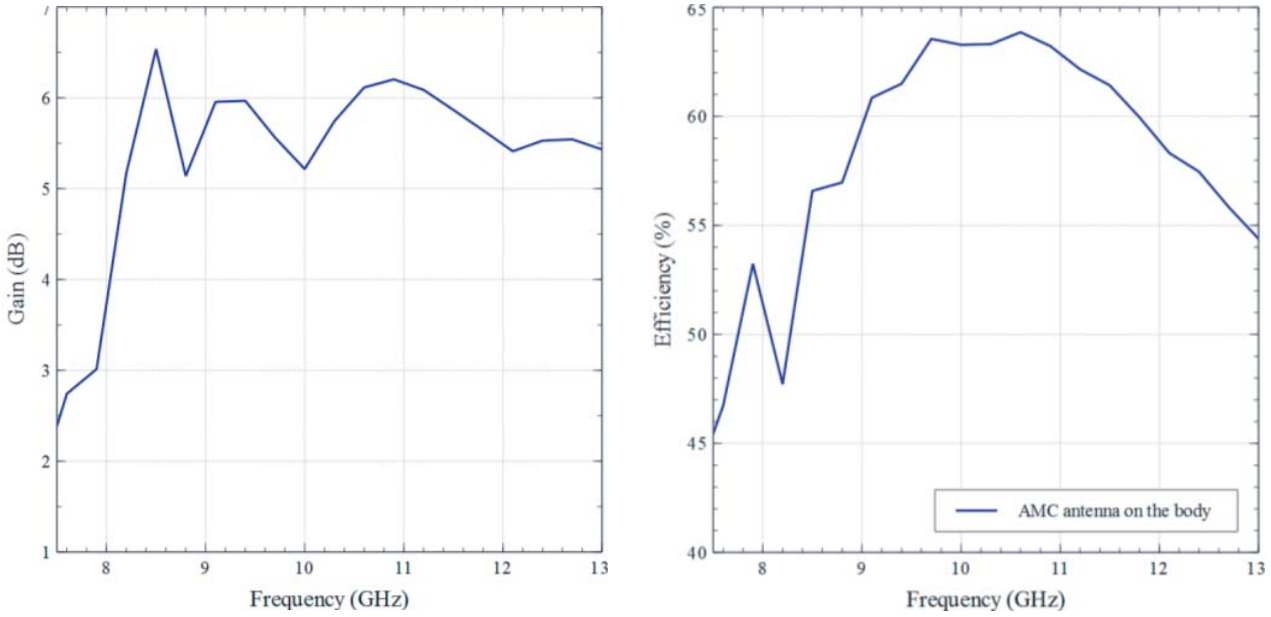

Figure 9. Simulated (a) gain of the AMC antenna on the body. (b) Efficiency of the monopole Antenna with AMC on the body.

They could come from the realization of the antenna because we had to superimpose several layers by agglomerating them with glue, which can cause additional losses. There is still an improvement in the total gain by 5 dB.

The radiation diagrams presented in Figures 8(a), (b), and (c) show good operation of the AMC at the three frequencies. We note an improvement in the gain in the direction perpendicular to the antenna. In addition, the rear radiation levels are lower for the antenna with AMC than the antenna alone, and we also note the same behavior when the AMC antenna is placed on the body as shown in Figure 8(d). The measurements of the antenna on AMC were made in an anechoic chamber of LEAT as shown in Figure 8(e). The gain and efficiency of the AMC antenna placed on the body, shown in Figure 9, are degraded compared to the AMC antenna placed in free space, due to interaction and even energy absorption in the body.

5. BENDING EFFECTS

The antennas are intended to be positioned under the body; they will therefore be subject to curvature constraints. To estimate the impact of curvatures on the antenna performance, we performed simulations along (Ox) axes of curvature with different radii. They are illustrated in Figure 10(a). The shape of the curvature is given according to that of a cylinder.

Figure 10(b) shows the reflection coefficient magnitude as a function of the curvature. It can be observed that the levels of reflection coefficient magnitudes are slightly lower than that of the plane reference antenna. These results demonstrate the robustness of the adaptation of the antenna even in a curved condition. The simulation time of the antenna with AMC is around a few minutes on a powerful simulator against the simulation on the body taking a few hours.

6. SPECIFIC ABSORPTION RATE

It is important to know the levels of radiation absorbed by the human body for antennas operating in emission; these levels must be lower than those given by the regulations [6]. Indeed, for medical

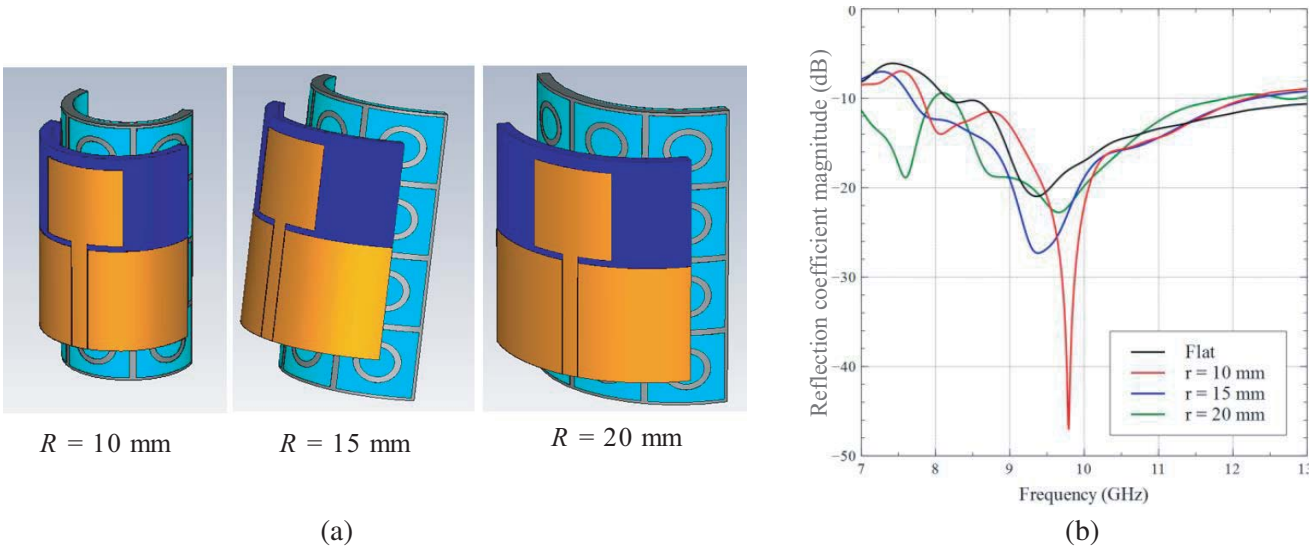

Figure 10. (a) Bending antenna. (b) Reflection coefficient magnitude of the bending antenna.

applications, the used antennas emit signals to detect a tumour at the skin level. If these antennas are near the human body, there will be interaction and even energy absorption in the latter. The distance between the phantom and the antenna is 5 mm. The SAR is expressed as follows:

$$\text{SAR} = \frac{\sigma E^2}{\rho} \tag{1}$$

where ρ is the volume density of the human body; σ is the conductivity of human tissues; and E is the electric field. We can observe, in Figure 11, areas where the SAR is concentrated, corresponding to the back radiation of the antenna. The maximum SAR reached here 0.102 W/kg for 1 gram of tissue. When considering electromagnetic radiation exposure standards that have a SAR of 1.6 W/kg, these values are well below the norm.

The discussed structure has been compared with other UWB antennas for medical applications given in [15–17], in terms of occupied area, bandwidth, reflection coefficient magnitude, and maximum gain. The results collected in Table 2 indicate that the proposed antenna outperforms the selected designs in terms of gain. Simultaneously, it offers a smaller size than compared structures.

Table 2. Summary of the dimensions, impedance bandwidth, reflection coefficient magnitude, and gain of designs given in the literature and of the proposed antenna.

Proposed design	Overall size of antenna width × length × height [mm^3]	−10 dB impedance bandwidth [GHz]	Minimum impedance matching of $\lvert S_{11}\rvert$ over the bandwidth [dB]	Maximum gain [dB]
[15]	50 × 50 × 1.5	3.1–10.6	−25	5
[16]	75 × 70 × 3	4–12	−30	3
[17]	30 × 40 × 1.524	4–12	−18	2
[19]	30 × 40 × 0.75	3–16	−30	5
Our proposed design	36 × 48 × 6.12	8.2–13	22	7.04

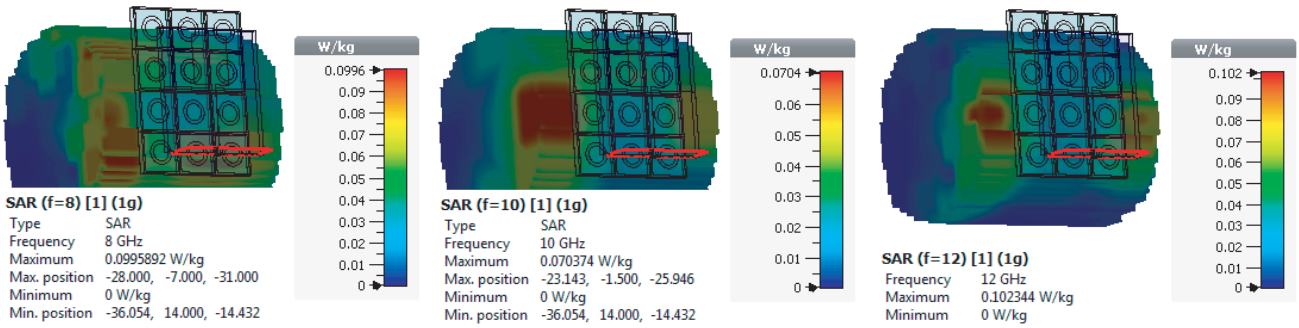

(a) (b) (c)

Figure 11. SAR at (a) 8 GHz, (b) 10 GHz, (c) 12 GHz.

7. CONCLUSION

In this work, we propose a miniature monopole antenna for an application in medical imaging which is the detection of skin cancer for a person affected by xeroderma pigmentosum disease. The antenna responds satisfactorily to the requirements imposed and exhibits UWB behavior. Indeed, the simulations using CST result in a reflection coefficient magnitude of -10 dB between 8 and 12 GHz. Simulations and measurements are in good agreement.

The radiation of this antenna has been analysed. It has good stability over the entire covered frequency band and at the two main planes E and H. The gain modest enough could be improved in future work by the networking of this antenna, although we consider it sufficient for the application in question given the proximity between the radiating element and the part of the human body that we must explore.

ACKNOWLEDGMENT

The authors are very thankful to Professor Jean-Marc Ribero for his valuable support and assistance during this work.

REFERENCES

1. Federal Communications Commission, "First report and order," Revision of Part 15 of the Commission's Rules Regarding Ultra-Wideband Transmission Systems, 2002, http://www.fcc.gov.
2. Neha, A. K., "Wearable antenna for skin cancer detection," *2nd International Conference on Next Generation Computing Technologies (NGCT-2016)*, 2016.
3. Natalia, R., "Ultra-Wide Band (UWB) and health applications," *IREAN Research Workshop*, Virginia Tech, 2005.
4. Caratelli, D., A. Massaro, R. Cingolani, and A. G. Yarovoy, "Accurate time-domain modeling of reconfigurable antenna sensors for non-invasive melanoma skin cancer detection," *IEEE Sensors Journal*, Vol. 12, No. 3, 635–643, Mar. 2012.
5. Jaleel, J. A., S. Salim, and R. B. Aswin, "Computer aided detection of skin cancer," *International Conference on Circuits, Power and Computing Technologies (ICCPCT)*, 1137–1142, Mar. 2013.
6. Sievenpiper, D., L. Zhang, R. Broas, N. Alexopoulos, and E. Yablonovitch, "High-impedance electromagnetic surfaces with a forbidden frequency band," *IEEE Transactions on Microwave Theory and Techniques*, Vol. 47, 2059–2074, Nov. 1999.
7. Khor, W. C., M. E. Bialkowski, A. Abbosh, N. Seman, and S. Crozier, "An ultra-wideband microwave imaging system for breast cancer detection," *International Symposium on Antennas and Propagation ISAP*, 1–5, 2006.

8. Joines, W. T., Y. Zhang, C. Li, and R. L. Jirtle, "The measured electrical properties of normal and malignant human tissues from 50 to 900 MHz," *Med. Phys.*, Vol. 21, No. 4, 547–550, Apr. 1994.
9. Chaudhary, S. S., R. K. Mishra, R. K. Mishra, A. Swarup, and J. M. Thomas, "Dielectric-properties of normal and malignant human breast tissues at radiowave and microwave-frequencies," *Indian J. Biochem. Biophys.*, Vol. 21, No. 1, 76–79, 1984.
10. Online: http://www.medisite.fr/dictionnaire-des-maladies-maladie-des-enfants-de-la-lune-xeroderma-pigmentosum.453831.5.html.
11. Prakash, P., M. P. Abegaonkar, A. Basu, and S. K. Koul, "Gain enhancement of a CPW-fed monopole antenna using polarizationinsensitive AMC structure," *IEEE Antennas and Wireless Propagation Letters*, Vol. 12, 1315–1318, 2013.
12. Wang, F. and T. Arslan, "A wearable ultra-wideband monopole antenna with flexible artificial magnetic conductor," *Loughborough Antennas & Propagation Conference (LAPC)*, 2016.
13. Malekpoor, H. and S. Jam, "Improved radiation performance of low profile printed slot antenna using wideband planar AMC surface," *IEEE Transactions on Antennas and Propagation*, Vol. 64, No. 11, 4626–4638, 2016.
14. Hadarig, R. C., M. E. de Cos, and F. L. Heras, "Novel miniaturized artificial magnetic conductor," *IEEE Antennas Wireless Propag. Lett.*, Vol. 12, 174–177, 2013.
15. Abbosh, A. M., "Directive antenna for ultrawideband medical imaging systems," *International Journal of Antennas and Propagation*, Vol. 2008, 6 pages, Article ID 854012, 2008.
16. Shanwar, A. R. and N. S. Othman, "UWB printed antenna for medical applications," *Proc. of the 2017 IEEE Region 10 Conference (TENCON)*, Malaysia, November 5–8, 2017.
17. Abdelhamid, M. M. and A. M. Allam, "Detection of lung cancer using ultra wide band antenna," *2016 Loughborough Antennas & Propagation Conference (LAPC)*, 2016.
18. Rahim, H. A., et al., "Measurement of dielectric properties of textile substrate," *Jurnal Teknologi (Sciences & Engineering)*, Vol. XX, No. 1, 1–6, 2015.
19. Sun, Y., T. I. Yuk, and S. W. Cheung, "Design of a textile ultra-wideband antenna with stable performance for body-centric wireless communications," *IET Microwaves, Antennas & Propagation*, Vol. 8, No. 15, 1363–1375, 2014, doi:10.1049/iet-map.2013.0658.
20. Mantash, M., A.-C. Tarot, S. Collardey, and K. Mahdjoubi, "Investigation of flexible textile antennas and AMC reflector," *International Journal of Antennas and Propagation*, Vol. 2012, 10 pages, Article ID 236505, 2012, doi:10.1155/2012/23650.